

See discussions, stats, and author profiles for this publication at: <https://www.researchgate.net/publication/221980364>

# Evaluation of High Resolution Magic-Angle Coil Spinning NMR Spectroscopy for Metabolic Profiling of Nanoliter Tissue Biopsies

ARTICLE in ANALYTICAL CHEMISTRY · MARCH 2012

Impact Factor: 5.64 · DOI: 10.1021/ac300153k · Source: PubMed

CITATIONS

17

READS

45

7 AUTHORS, INCLUDING:



[Alan Wong](#)

French National Centre for Scientific Research

65 PUBLICATIONS 1,401 CITATIONS

[SEE PROFILE](#)



[Beatriz Jiménez](#)

Imperial College London

29 PUBLICATIONS 460 CITATIONS

[SEE PROFILE](#)



[Elaine Holmes](#)

Imperial College London

476 PUBLICATIONS 28,801 CITATIONS

[SEE PROFILE](#)



[Jeremy K Nicholson](#)

Imperial College London

754 PUBLICATIONS 43,253 CITATIONS

[SEE PROFILE](#)

# Evaluation of High Resolution Magic-Angle Coil Spinning NMR Spectroscopy for Metabolic Profiling of Nanoliter Tissue Biopsies

Alan Wong,<sup>†</sup> Beatriz Jiménez,<sup>‡</sup> Xiaonan Li,<sup>†</sup> Elaine Holmes,<sup>‡</sup> Jeremy K. Nicholson,<sup>‡</sup> John C. Lindon,<sup>\*,‡</sup> and Dimitris Sakellariou<sup>\*,†</sup>

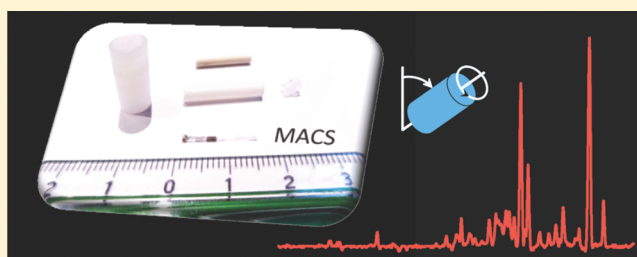
<sup>†</sup>CEA Saclay, DSM, IRAMIS, UMR CEA/CNRS no 3299 – SIS2M, Laboratoire Structure et Dynamique par Résonance Magnétique, F-91191, Gif-sur-Yvette Cedex, France

<sup>‡</sup>Division of Biomolecular Medicine, Department of Surgery and Cancer, Faculty of Medicine, Imperial College London, SW7 2AZ, London, United Kingdom

## S Supporting Information

**ABSTRACT:** High-resolution magic-angle sample spinning (HR-MAS) <sup>1</sup>H NMR spectroscopy of tissue biopsies combined with chemometric techniques has emerged as a valuable methodology for disease diagnosis and environmental assessments. However, the tissue mass required for such experiments is of the order of 10 mg, and this can compromise the metabolic evaluation because of tissue heterogeneity. Tissue availability is often a limitation for clinical studies due to histopathological requirements, which are currently the gold standard for diagnosis, for example, in the case of tumors.

Here, we introduce the use of a rotating micro-NMR detector that optimizes the coil filling factor such that mass-limited samples can be measured. We show the results for measuring nanoliter volume tissue biopsies using a commercial HR-MAS probe for the first time. The method has been tested with bovine muscle and human gastric mucosal tumor tissue samples. The gain in mass sensitivity is approximate up to 17-fold, and the adequate spectral resolution (3 Hz) allows the measurement of the metabolite profiles in nanoliter volume samples, thereby limiting the ambiguity resulting from heterogeneous tissues; thus, the approach presents diagnostic potential for studies by metabolomics of mass-limited biopsies.



High-resolution magic-angle sample spinning (HR-MAS) NMR spectroscopy is now recognized as a routine practice technique for investigating metabolic profiles in intact tissues.<sup>1,2</sup> The capability of precise characterization of biochemical and metabolic profiles in tissues offers the possibility of the use of HR-MAS NMR as a clinical diagnostic tool.<sup>3,4</sup> As tissues are not isotropic samples, residual anisotropic interactions can appear in the spectra. HR-MAS eliminates the line broadenings associated from residual dipolar couplings, some diamagnetic susceptibility effects, and  $B_0$  field inhomogeneity in the sample, by rapid sample spinning at the magic-angle ( $54.74^\circ$ ) with respect to the static magnetic field. HR-MAS NMR studies provide a number of advantages over the traditional high-resolution liquid-state NMR of tissue extracts: (i) they allow the study of metabolites in the real structure of the tissue potentially providing information on molecular mobility and compartmentation; (ii) they require no sample preparation and thus no sample destruction; (iii) tissue extractions often require a large quantity of sample;<sup>5</sup> and (iv) the extraction procedures often provide selective profiles because they can discriminate metabolites on the basis of their solubility in a particular solvent.

Nowadays, cancer diagnosis is mainly achieved initially on the basis of radiological image information and the identification of tumor markers in blood tests. Depending on the

nature of the disease, the radiological analysis can provide an inaccurate diagnosis. In some exploratory studies, such as colonoscopic examinations for colon cancer, small tissue biopsies can be collected from the presumed affected tissue, but often, the entire amount of available tissue is used for histopathological analysis and further biochemical tests on the sample are unable to be performed. There is thus a need for methods that can provide detailed biochemical analyses of very small amounts of tissue. Another advantage of the use of smaller biopsy samples is the reduced tissue heterogeneity and the increased ability to observe single cell types and thus to localize the biomarkers associated with each cell type.

Besides human studies, metabolomics is also widely applied in rodent models for disease assessment, as well as pharmaceutical or toxicological studies. In these cases, the organs of interest sometimes are limited in size, making such tissue difficult to study by HR-MAS. Another application of HR-MAS NMR in metabolomics is in vitro cell studies, where obtaining a sufficient volume of cells can be a challenge. For NMR to continue as a front line analytical platform in metabolomics, the ability to generate high quality data from

Received: January 16, 2012

Accepted: March 22, 2012

Published: March 22, 2012



smaller (micro- and possible nanoscale) sample volumes is critical.

The intrinsically low NMR sensitivity is a formidable test for small tissue volume detection with HR-MAS. One common approach for increasing the sensitivity is the use of a higher magnetic field. Ultrahigh field magnet technology has now reached 1 GHz for  $^1\text{H}$  observation,<sup>6</sup> but the cost of the system is unreachable for most laboratories. Moreover, a faster sample spinning frequency is required for eliminating the peak-obstructing spinning sidebands from the spectral window (0–10 ppm for  $^1\text{H}$ ). This would also increase the centrifugal effect of the spinning on the tissues and could lead to tissue damage. An alternative approach for sensitivity enhancement is the use of micro-NMR detectors. Olson et al.<sup>7</sup> have demonstrated the high performances of nanoliter liquid NMR detection using a microsolenoid coil, herein termed as a “microcoil”. Microcoil detection is now a common approach for NMR spectroscopy of organic liquids and biofluids and has triggered the development of high-throughput technology.<sup>8</sup> Moreover, the microcoil application for liquid NMR has already pushed forward with hyphenation to liquid-chromatography in metabonomics<sup>9</sup> and with microfluidic devices as a promising cancer diagnostic magnetic resonance sensor.<sup>10</sup> However, the microdetection for tissue biopsies with HR-MAS is nearly nonexistent due to the technical challenges for sample spinning without destroying the sensitivity and resolution. Recently, a rotating micro-NMR detector has been developed for solid materials.<sup>11,12</sup> It has been called a magic angle coil spinning (MACS) microcoil. It is a small resonant solenoid coil and can be wirelessly excited and detected using resonant-inductive coupling to commercial cross-polarization MAS (CP-MAS) or HR-MAS probes. The fact that the microsolenoid rotates together with the sample at the magic-angle inside a MAS stator permits high-resolution NMR spectroscopy of solids and semisolids. The MACS approach has already been applied to tissues using a solid-state CP-MAS probe, and although this probe is not optimal for high-resolution spectroscopy, a tremendous mass sensitivity gain was demonstrated, up to 2 orders of magnitude, for nanoliter samples.<sup>11,13</sup> However, the spectral resolution limit has yet to be investigated for metabonomic studies.

Since MACS can be readily adapted to any MAS probes, here, we present a study of the MACS technology to metabolic profiling in bovine and human tissues using a commercial HR-MAS probe, designed for high-resolution NMR acquisitions.<sup>14</sup> We examine both sensitivity and resolution limits with the MACS detection in real samples.

## EXPERIMENTAL METHODS

**MACS Fabrication.** A schematic diagram of the MACS microcoil is shown in Figure 1. Each coil was constructed by manually winding a solenoid from a 62  $\mu\text{m}$  diameter coated copper wire around a 870/700  $\mu\text{m}$  (outer/inner diameter) quartz capillary with 12–14 turns, and this coil was soldered to a nonmagnetic 2.4 pF capacitor to give a target frequency at  $400 \pm 20$  MHz for  $^1\text{H}$  detection. The quality factor was between 55 to 60. The detection sample volume was about 690 nL.

In order to make the MACS microcoil rapidly spin in the HR-MAS probe, it was tightly fitted inside a custom-made three-chamber Shapal-M ceramic insert (see Figure 1) designed to fit snugly inside a standard 4 mm Bruker rotor, which allows for an ensemble rotation with the microcoil. The three chambers have different diameter sizes to fit the capacitor,

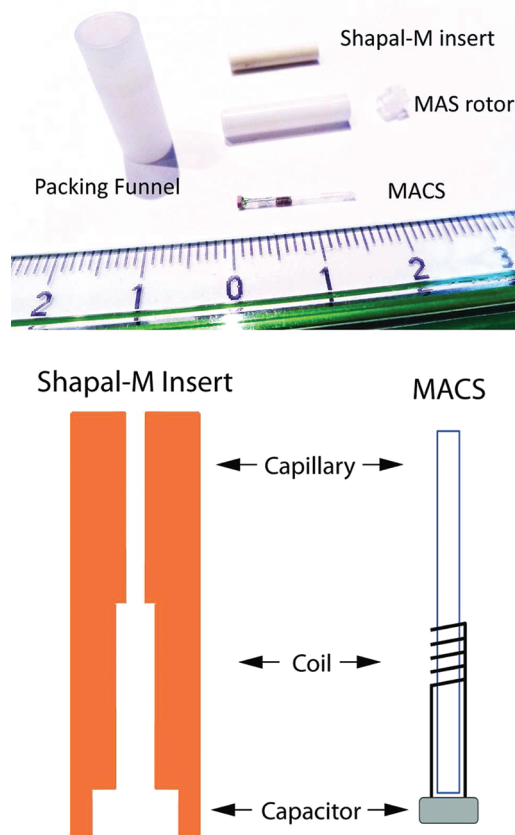


**Figure 1.** (Top) Photographic image of a MACS microcoil, a bespoke packing funnel, and a 4 mm Bruker MAS rotor. (Bottom) Schematic diagram of a three-chamber Shapal-M insert and a MACS microcoil, showing the three different regions for quartz capillary, copper solenoid coil, and ceramic capacitor. A tight fit between the MACS and insert and between insert and rotor is essential for stable rapid spinning.

copper coil, and capillary portions of the microcoil. Furthermore, the ceramic insert was made of aluminum nitride (Shapal-M), allowing heat dissipation from the eddy currents generated by the coil spinning inside the magnet.<sup>15</sup>

**Test Solution.** An initial test solution of 2 mM sucrose in  $\text{D}_2\text{O}$  (Goss Scientific Instruments Ltd., Nantwich, UK) was used for trial experiments in order to set the tuning, pulse, and initial shimming parameters. The sucrose solution was introduced into the MACS microcoil using a microsyringe, avoiding the formation of bubbles inside the capillary. The microcoil was subsequently closed using wax that was melted inside the capillary to ensure a seal.

**Tissue Preparation.** For this evaluation, samples of bovine muscle (obtained commercially) and human tumor from gastric mucosa were used. The human tissue was obtained as part of an ongoing study, and all necessary ethical procedures and approvals were in place. The sample preparation for MACS is similar to the procedures for a 4 mm rotor.<sup>2</sup> Due to the small quantity of tissue sample, a custom-made Kel-F funnel (15 mm in length  $\times$  5 mm in diameter) was used for packing the tissue into a small diameter capillary (Figure 1). The design and function of the Kel-F funnel are identical to that of the commercial funnel used for packing solid powders. Frozen tissues were taken from a 193 K freezer and placed in an ice bath while packing. The capillary was then filled with  $\text{D}_2\text{O}$ –

saline solution (9%) using a fine-needle syringe to ensure no air bubbles and gaps in the sample regions. The capillary was then sealed with paraffin wax to prevent leakage during the sampling spinning. The entire sample preparation for MACS took about 5–10 min. A disposable 2 mm biopsy punch was used for packing the bulk tissue (16 mg) into a 30  $\mu$ L Kel-F insert following the standard protocols.<sup>2</sup>

**NMR Spectroscopy.**  $^1\text{H}$  NMR experiments were carried out on a narrow-bore 9.4 T Bruker (Rheinstetten, Germany) Avance III spectrometer operating at a  $^1\text{H}$  frequency of 400.132 MHz, with a Bruker 4 mm  $^1\text{H}/^{13}\text{C}/^2\text{H}$  HR-MAS probe. Spectra were acquired with sample spinning frequency either at 1360 or  $4500 \pm 2$  Hz and with the rotor temperature maintained at either 5 or  $15 \pm 0.2$  °C. A field-lock signal was provided by the  $^2\text{H}$  resonance of the HDO in all experiments. The  $B_0$  field homogeneity, required for adequate spectral resolution, was achieved by a shimming procedure specific for MAS.<sup>16</sup> The shimming was performed under sample spinning and by monitoring the HDO signal. The sampling spinning rendered a simplified shimming procedure, mainly using the Z, X,  $X^2 - Y^2$ , ZX,  $Z^3$ , and  $Z(X^2 - Y^2)$  shims. A full-width-at-half-maximum (fwhm) of 3–8 Hz was obtained for the natural abundance  $^1\text{H}$  NMR signal arising from protons in HDO, and this was readily achieved for all samples under MACS. A continuous irradiation during the recycling delay was applied in all experiments to suppress the water signal. Experiments acquired included 1D presaturation, 1D NOESY (Nuclear Overhauser Effect Spectroscopy) with presaturation and CPMG (Carr–Purcell–Meiboom–Gill), and 2D TOCSY (TOtal Correlation Spectroscopy) using standard pulse sequences. Recycling delays were 1 or 2 s for all 1D experiments with acquisition times ranging between 1.3 and 2.7 s. A spectral width of 6410 Hz was used. The total 1D acquisition time for the sucrose solution was 1.9 h and for both muscle and mucosa tissues was 1.4 h. 1D NMR spectra were processed with zero-filling and apodization functions (negative exponential or Lorentzian–Gaussian transformation) prior to Fourier transformation to enhance the spectral resolution or signal-to-noise ratio.<sup>17</sup> For tissues, the chemical shifts were referenced to that of the internal alanine methyl doublet signal at 1.47 ppm.

## RESULTS AND DISCUSSION

**Nanoliter Detections of Sucrose Solution.** To demonstrate the spectral resolution acquired with MACS using HR-MAS, we acquired a  $^1\text{H}$  spectrum of 692 nL of 2 mM sucrose/ $\text{D}_2\text{O}$ . The spectrum is shown in Figure 2a. After the shimming procedure described above, the fwhm of the HDO signal was consistently found in the range of 3–8 Hz, suggesting that this is the spectral resolution limit for the current MACS design. An enhanced resolution spectrum, Figure 2b, was achieved by applying a Gaussian apodization function prior to Fourier transformation and the resolution-enhanced spectrum was in very good agreement with the spectrum acquired from a 30  $\mu$ L sample of 2 mM sucrose in  $\text{D}_2\text{O}$  in disposable insert introduced in a conventional HRMAS rotor with a static coil (Figure 2c). The metabolic profile of sucrose is very well-defined. Signals belonging to the glucose protons present a clear multiplicity with measurable  $J$ -couplings (see Table 1 and Figure 2). These are,  $\text{H}_2^g$  at 5.47 ppm (doublet),  $\text{H}_3^g$  at 3.58 ppm (doublet of doublets),  $\text{H}_4^g$  at 3.78 ppm (triplet), and  $\text{H}_5^g$  at 3.48 ppm (triplet). Protons  $\text{H}_2^f$  and  $\text{H}_3^f$  from the fructose unit, 4.06 ppm (triplet) and 4.22 ppm (doublet), respectively, are also easily

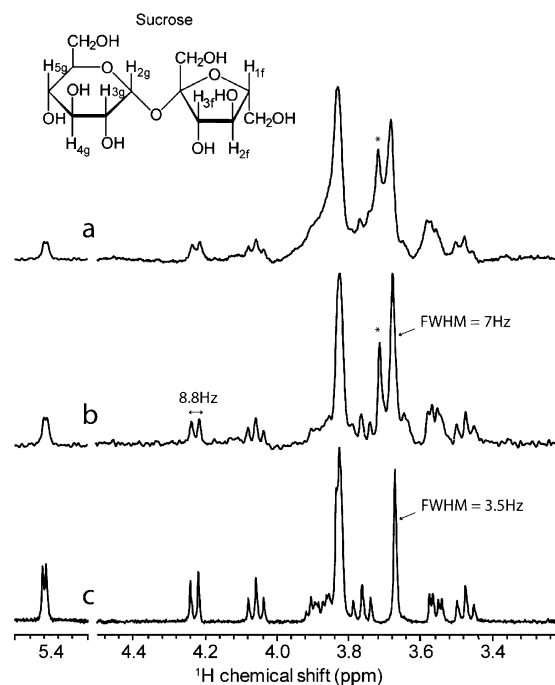


**Figure 2.** 1D  $^1\text{H}$  water-suppressed NMR spectra of 2 mM sucrose in  $\text{D}_2\text{O}$  acquired with (a, b) a 692 nL MACS microcoil (3072 scans) and (c) a 30  $\mu$ L Kel-F insert. The associated molecule structure is shown on the top left corner. Labels on the structure correspond to the text. Spectra (a) and (b) are processed from the same data but applying different apodization functions: (a) LB = 1 Hz of exponential and (b) LB = -2 Hz of Gaussian with GB = 0.1. Clearly, Gaussian apodization provides an enhanced resolution spectrum with a good compromise for the signal-to-noise ratio.<sup>17</sup> The asterisk indicates the presence of a wax impurity.

**Table 1. Coupling Constant Values for Sucrose Spectra Acquired in a Conventional 30  $\mu$ L Teflon HR-MAS Insert, in a 692 nL Glass MACS Insert, and Obtained from the Literature<sup>a</sup>**

assignment	chemical shift (ppm)	multiplet <sup>b</sup>	HR-MAS $J$ (Hz)	MACS $J$ (Hz)	literature/liquid NMR <sup>6</sup>
$\text{H}_2^g$	5.47	d	3.9	3.4	3.89
$\text{H}_3^g$	3.58	dd	9.8/3.9	10.4/4.7	9.98/3.89
$\text{H}_4^g$	3.78	t	9.6	9.6	9.57
$\text{H}_5^g$	3.48	t	9.4	9.5	9.30
$\text{H}_2^f$	4.06	t	8.6	8.5	8.59
$\text{H}_3^f$	4.22	d	8.8	8.8	8.75

<sup>a</sup>See Figure 2 for proton nomenclature. <sup>b</sup>Abbreviations and key: d, doublet; dd, doublet of doublets; t, triplet.

identified. The essentially uncoupled singlet at 3.67 ppm from the methylene  $\text{H}_6^f$  of the fructose moiety has a line width of 7 Hz compared to the ca. 3 Hz resolution for the HR-MAS spectrum. It should be pointed out that the observed spectral resolution in Figure 2 is a marked improvement over that of the currently available approaches to microdetection with MAS, either using inductively coupled spinning microcoils (MACS)<sup>11,13</sup> or using a static microcoil in a piggy-back MAS approach.<sup>18</sup> Since the microcoil is static in the latter approach, the coil susceptibility is not averaged by the sample spinning. Thus, good shimming can be difficult to achieve in that case and can hinder high resolution acquisitions. Similar effects are well-known in static microcoils for liquid-state  $^1\text{H}$  studies.<sup>19</sup> On



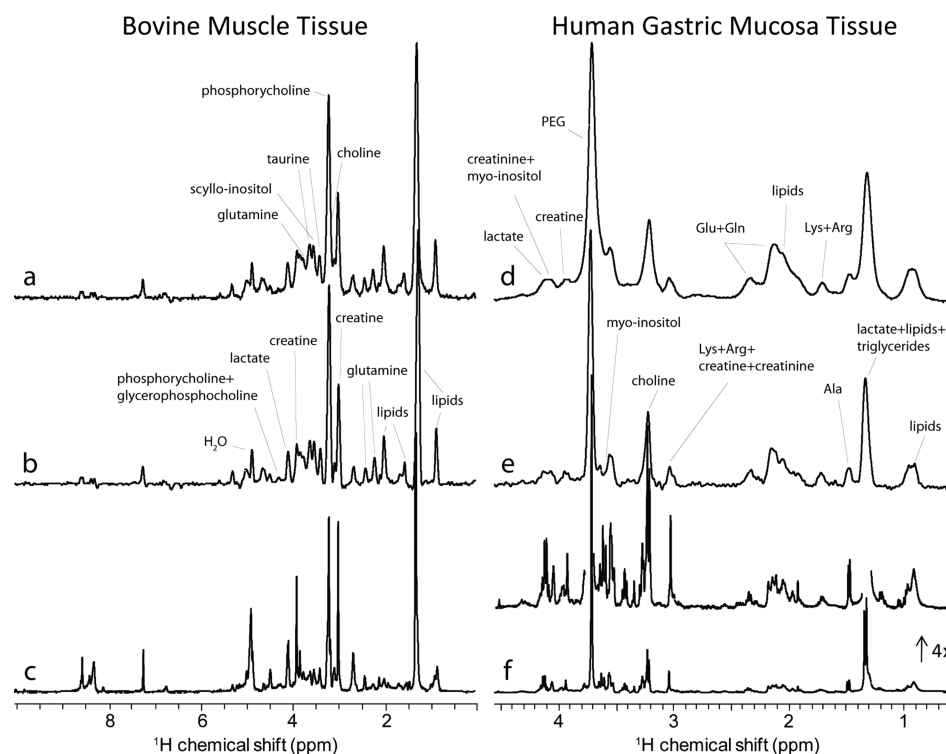


**Figure 3.** 1D  $^1\text{H}$  water suppression CPMG- $T_2$ -filter NMR spectra of (a–c) bovine muscle tissue and (d–f) human gastric mucosa tumor tissue. (a,b and d,e) were acquired with a 692 nL MACS microcoil, and (c and f) were with a 30  $\mu\text{L}$  Kel-F insert. Spectra (a and b) and (d and e) are processed from the same data but applying different apodization functions: (a,d) LB = 1 Hz of exponential and (b,e) LB = 5 Hz of Gaussian with GB = 0.015. Complete peak assignments for both tissues are reported in the Supporting Information. In (f), the top spectrum is scaled by a factor of 4 to reveal the weak metabolite signals.

the other hand, when the MACS microcoil spins rapidly together with the sample at the magic-angle, it averages the radial field inhomogeneities and offers a simpler shimming procedure. In comparison, the previously published studies using MACS<sup>11,13</sup> were conducted with a solid-state CP-MAS NMR probe and resulted in 15–40 Hz line widths.

The sucrose mass quantity present in the 30  $\mu\text{L}$  disposable insert is 20.5  $\mu\text{g}$ , while the MACS coil has a volume of 692 nL and contains 474 ng of sucrose. The HR-MACS experiment shown in Figure 2 has a Signal to Noise Ratio<sup>20</sup> (S/N) of 7.6 with 116 min acquisition, while the HR-MAS experiment has a S/N of 19.4 with a 4.9 min acquisition. For the same sucrose quantity contained in the HR-MACS coil (474 ng), the S/N for the HR-MAS probe would decrease by a factor of 43, resulting in a S/N value of just 0.45. In other words, a factor of 17 in S/N is lost. In order to obtain the same S/N to that of the HR-MACS spectrum in Figure 2, the acquisition time would need to last 23 h. This is nearly 12 times longer compared to the 1.9 h acquisition achieved using the MACS detector. Therefore, with the MACS detector, the data acquisition using submilligram quantities of tissue is now possible, and this is especially important for biopsy samples where physical and metabolic changes can occur during long acquisition period. With this gain in mass sensitivity, 2D NMR spectroscopy also becomes feasible, and to demonstrate this, a  $^1\text{H}$ – $^1\text{H}$  TOCSY spectrum (see Supporting Information) was acquired with the MACS detector.

**Nanoliter Detection of Tissues.** Figure 3 shows the 1D CPMG- $T_2$ -weighted  $^1\text{H}$  spectra of two different tissues: (a–c) bovine muscle and (d–f) human gastric mucosa tumor tissue. The spectral profile (i.e., individual peak positions and

intensities), shown in Figure 3b, acquired with the 690 nL microcoil filled with a crude approximate 500 ng of muscle tissue is in excellent agreement with the spectrum, Figure 3c, acquired with a regular 4 mm rotor containing a 30  $\mu\text{L}$  disposable insert packed with 16 mg of tissue. The gain in mass sensitivity for muscle is estimated to be about 7-fold (note: the MACS coil used for the tissue is not at an optimal comparison to that for sucrose, thus lower gain is observed). Nonetheless, the observed sensitivity gain means that to obtain the same S/N ratio using the regular 4 mm HR-MAS rotor packed with just 500 ng of muscle tissue, the acquisition time should be increased from 1 h 15 min to almost 9 h. The metabolic spectral profile of the tissues is apparent and allows complete peak assignments (detailed assignments are presented in the Supporting Information). The potential of MACS for the analysis of nanoliter samples has already been shown using a broadband spectrometer,<sup>13</sup> but the inherited low resolution of the spectrum did not provide a very recognizable profile for tissue. For the first time, metabolites other than lipids and the residual water are unambiguously observed and identified in nanoliter tissues.

Figure 3d–e shows the CPMG spectra of nanoliter human gastric mucosa tumor tissue. This was chosen because it is a typical human tissue sample from a situation where tissue is in very limited supply (e.g., from a colonoscopic procedure). The acquired spectral resolution is not as good as in those of the muscle tissue. Nonetheless, the spectral profile corresponds well with the bulk sample (Figure 3f) and allows the identification of the major metabolites present in the tissue (see Supporting Information). It should be noted that the large singlet at 3.71 ppm appears in both the spectra of the nanoliter

and bulk sample and corresponds to polyethylene glycol (PEG), which is a component of a number of laxatives, typically used in bowel preparation before surgery procedures.

Enhancement in mass sensitivity is not the sole advantage for the MACS detection. The small sample volume diameter in MACS minimizes the centrifugal forces ( $F = m\omega^2r$ , where  $m$  is the mass,  $\omega$  is the spinning frequency, and  $r$  is the radius from the rotation axis) exerted upon the tissues and helps to preserve the tissue integrity. For example, decreasing the sample volume diameter from 1.9 mm (30  $\mu$ L Kel-F insert) to 0.7 mm (MACS) decreases the centrifugal forces exert upon the tissues by a factor of 3. This could be a very important advantage for analysis of softer tissues such as brain<sup>21</sup> and for ultrahigh field NMR detection, where higher spinning frequency is usually required to move the spinning sidebands away from the metabolite spectral region (0–10 ppm). A final major advantage of the use of nanoliter volume tissues is overcoming the intrinsic biological heterogeneity of tissue samples. The study of smaller sample masses will allow examination of more specific types of cells such as that seen in normal tissue, tumor tissue, and tumor margins and one to obtain more biochemically relevant information than currently available using standard NMR-based metabolic profiling methodology.

## ■ CONCLUDING REMARKS

The study presented here demonstrates that the currently designed MACS microcoil can provide excellent mass sensitivity and reasonable resolution for metabolic profiling of nanoliter biopsies. Despite the spectral resolution (3 Hz line width) from MACS being somewhat poorer compared to the standard <1 Hz from conventional HR-MAS spectra, the resultant spectra still offer reasonable resolution for metabolite identification. Several data processing options including reference deconvolution and other resolution enhancement techniques could be already applied successfully on the NMR spectra obtained by MACS. Resolution is nevertheless of prime importance in metabolic studies and the residual line width of MACS should be further reduced. One source of the line broadening is the magnetic susceptibility gradients in the MACS components, i.e., the glass capillary, adhesive glue, copper wire, ceramic capacitor and solder, each of which have different susceptibilities. Eliminating some of these components could minimize the gradients and provide a more uniformly distributed magnetic susceptibility MACS microcoil, and hence, better shimming could be achieved.<sup>14</sup> Another option to reduce the line width is by casing the MACS microcoil into a solid susceptibility matched material.<sup>22</sup> An additional source of the line broadening is temperature gradients at the sample location originating from the eddy currents developed in the spinning microcoil: a temperature gradient of 0.5 degrees could lead to 3.2 Hz of line width for water at 400 MHz. Temperature effects have been measured in MACS<sup>15</sup> and can be controlled by microfabrication procedures. The relative importance between these two sources is currently under theoretical and experimental investigation.

The assessment of the reproducibility of the MACS experiments is a related issue that can come from the microcoil detectors as well as from the sample itself, even if taken from the same aliquot. The coils being manually wound are not completely identical, nor are the chip capacitors (the best ceramic capacitor capacitance tolerances are of the order of 5% to 10%) used for their tuning. This leads to a nonreproducible radio frequency (and finally sensitivity) performance. We are

about to perform long systematic studies about the fabrication reproducibility, but our experience on liquid samples showed that this leads to only a  $\pm 5\%$  variation in sensitivity, because the ensemble is fine-tuned and matched by the capacitors of the HRMAS probe. Furthermore, the semisolid tissue samples are heterogeneous. Because the sample volume is very small, we cannot guarantee that exactly the same volume or type of tissue is sampled. In the future, we will need to perform histological studies on the samples we detect in order to validate the reproducibility of the sample. This direction is currently followed, but it will require some time.

The gold standard in clinical tissue assessment nowadays is histopathology. When the quantity of tissue obtained from a single biopsy is limited, the 10 mg required to perform a regular HR-MAS NMR analysis can be difficult to obtain, as it can compromise conventional histopathological assessments. However, if the amount of tissue required to obtain the same NMR information is reduced to the submilligram level, then there would be no compromise. Moreover, it enables enriching the biochemical information from a single tissue biopsy and offers an improved disease assessment.<sup>23</sup> Another area where MACS could also be of benefit, besides human or animal studies, is examination of single small organisms. For example, the early stages of *Drosophila lava* and *Caenorhabditis elegans* are submillimeter size organisms, and each single organism could readily be fitted inside a MACS microcoil for analysis. The latter has already been investigated with HR-MAS NMR spectroscopy but only by combining large quantities of *C. elegans* for a single measurement.<sup>24</sup> The mass sensitivity demonstrated here indicates that single organism spectroscopy is feasible. Another possible application for MACS could be the study of scarce in vitro cells. For example, in stem cell cultures, the HR-MAS study of intact cells might be challenging because obtaining sufficient cells for a 30  $\mu$ L volume HR-MAS spectrum might imply introducing a certain percentage of spontaneously differentiated cells.<sup>25</sup> We anticipate the nanoliter MACS detector could play a vital role and open a framework in metabonomics NMR for precious biopsies.

## ■ ASSOCIATED CONTENT

### Supporting Information

Four figures and one table presenting the full metabolic profile assignment of the tissue analyzed in the paper. This material is available free of charge via the Internet at <http://pubs.acs.org>.

## ■ AUTHOR INFORMATION

### Corresponding Author

\*Tel: +44 (0)20 7594 3194 (J.C.L.); +33 1 69 08 11 26 (D.S.).  
Fax: +44 (0)20 7594 3066 (J.C.L.); +33 1 69 08 98 06 (D.S.).  
E-mail: [j.lindon@imperial.ac.uk](mailto:j.lindon@imperial.ac.uk) (J.C.L.); [dsakellariou@cea.fr](mailto:dsakellariou@cea.fr) (D.S.).

### Notes

The authors declare no competing financial interest.

## ■ ACKNOWLEDGMENTS

A.W. and B.J. contributed equally to this work. The research leading to these results has received funding from the European Research Council under the European Community's Seventh Framework Programme (FP7/2007-2013): ERC grant agreement # 205119 and the Biomedical Research Council (UK). We would like to thank Angelo Guiga (CEA, France) for machining the Shapal-M inserts for MACS.

## ■ REFERENCES

- (1) Lindon, J. C.; Beckonert, O. P.; Holmes, E.; Nicholson, J. K. *Prog. Nucl. Magn. Reson. Spectrosc.* **2009**, *55*, 79–100 and references therein.
- (2) Beckonert, O.; Coen, M.; Keun, H. C.; Wang, Y.; Ebbels, T. M. D.; Holmes, E.; Lindon, J. C.; Nicholson, J. K. *Nat. Protoc.* **2010**, *5*, 1019–1032.
- (3) Sitter, B.; Bathen, T. F.; Tessem, M. B.; Gribbestad, I. S. *Prog. Nucl. Magn. Reson. Spectrosc.* **2009**, *54*, 239–254 and references therein.
- (4) Cheng, L. L.; Ma, M. J.; Becerra, L.; Ptak, T.; Tracey, I.; Lackner, A.; Conzalex, R. G. *Proc. Natl. Acad. Sci. U.S.A.* **1997**, *94*, 6408–6413.
- (5) Beckonert, O.; Keun, H. C.; Ebbels, T. M. D.; Bundy, J.; Holmes, E.; Lindon, J. C.; Nicholson, J. K. *Nat. Protoc.* **2010**, *5*, 1019–1032.
- (6) Bhattacharya, A. *Nature* **2010**, *463*, 605–606.
- (7) Olson, D. L.; Peck, T. L.; Webb, A. G.; Magin, R. L.; Sweedler, J. V. *Science* **1995**, *270*, 1967–1970.
- (8) Grimes, J. H.; O'Connell, T. M. *J. Biomol. NMR* **2011**, *49*, 297–305.
- (9) Albert, K. *On-line LC-NMR and related technologies*; Wiley: Chichester, 2002.
- (10) Lee, H.; Yoon, T.-J.; Figueiredo, J.-L.; Swirski, F. K.; Weissleder, R. *Proc. Natl. Acad. Sci. U.S.A.* **2009**, *106*, 12459–12464.
- (11) Sakellariou, D.; Le Goff, G.; Jacquinot, J.-F. *Nature* **2007**, *447*, 694–697.
- (12) Jacquinot, J.-F.; Sakellariou, D. *Concepts Magn. Reson., Part A* **2011**, *38*, 33–51.
- (13) Wong, A.; Aguiar, P. M.; Sakellariou, D. *Magn. Reson. Med.* **2010**, *63*, 269–274.
- (14) Doty, F. D.; Entzminger, G.; Yang, Y. A. *Concepts Magn. Reson., Part A* **1998**, *10*, 239–260.
- (15) Aguiar, P. M.; Jacquinot, J.-F.; Sakellariou, D. *J. Magn. Reson.* **2009**, *200*, 6–14.
- (16) Piotto, M.; Elbayed, K.; Wieruszkeski, J.-M.; Lippens, G. *J. Magn. Reson.* **2005**, *173*, 84–89.
- (17) Lindon, J. C.; Ferrige, A. G. *Prog. Nucl. Magn. Reson. Spectrosc.* **1980**, *14*, 27–66.
- (18) Janssen, H.; Brinkmann, A.; van Eck, E. R. H.; van Benthum, J. M.; Kentgens, A. P. M. *J. Am. Chem. Soc.* **2006**, *128*, 8722–8723.
- (19) Webb, A. G. *Prog. Nucl. Magn. Reson. Spectrosc.* **1997**, *31*, 1–42.
- (20) Hoult, D. I.; Richards, R. E. *J. Magn. Reson.* **1976**, *24*, 71–85.
- (21) Martínez-Bisbal, M. C.; Esteve, V.; Martínez-Granados, B.; Celda, B. *J. Biomed. Biotechnol.* **2011**, 1–8.
- (22) De Zanche, N.; Barmet, C.; Nordmeyer-Massner, J. A.; Pruessmann, K. P. *Magn. Reson. Med.* **2008**, *60*, 176–186.
- (23) Chan, E. C.; Koh, P. K.; Mal, M.; Cheah, P. Y.; Eu, K. W.; Backshall, A.; Cavill, R.; Nicholson, J. K.; Keun, H. C. *J. Proteome Res.* **2009**, *8*, 352–361.
- (24) Blaise, B. J.; Giacomotto, J.; Bénédicte, E.; Dumas, M.-E.; Toulhoat, P.; Ségalat, L.; Emsley, L. *Proc. Natl. Acad. Sci. U.S.A.* **2007**, *104*, 19808–19812.
- (25) MacIntyre, D. A.; Melguizo Sanchis, D.; Jiménez, B.; Moreno, R.; Stojkovic, M.; Pineda-Lucena, A. *PLoS One* **2011**, *6*, e16732.
- (26) Wishart, D. S.; Knox, C.; Guo, A. C.; Eisner, R.; Young, N.; Gautam, B.; Hau, D. D.; Psychogios, N.; Dong, E.; Bouatra, S.; Mandal, R.; Sinelnikov, I.; Xia, J.; Jia, L.; Cruz, J. A.; Lim, E.; Sobsey, C. A.; Shrivastava, S.; Huang, P.; Liu, P.; Fang, L.; Peng, J.; Fradette, R.; Cheng, D.; Tzur, D.; Clements, M.; Lewis, A.; De Souza, A.; Zuniga, A.; Dawe, M.; Xiong, Y.; Clive, D.; Greiner, R.; Nazyrova, A.; Shaykhtudinov, R.; Li, L.; Vogel, H. J.; Forsythe, I. *Nucleic Acids Res.* **2009**, *37*, D603–10.

# Evaluation of High Resolution Magic-Angle Coil Spinning NMR Spectroscopy for Metabolic Profiling of Nanoliter Tissue Biopsies.

Supplementary Materials

*Alan Wong,<sup>†,§</sup> Beatriz Jiménez,<sup>‡,§</sup> Xiaonan Li,<sup>†</sup> Elaine Holmes,<sup>‡</sup> Jeremy K. Nicholson,<sup>‡</sup> John  
C. Lindon,<sup>‡\*</sup> Dimitris Sakellariou.<sup>†\*</sup>*

<sup>†</sup> CEA Saclay, DSM, IRAMIS, UMR CEA/CNRS no 3299 – SIS2M, Laboratoire Structure et  
Dynamique par Résonance Magnétique, F-91191, Gif-sur-Yvette Cedex, France.

<sup>‡</sup> Division of Biomolecular Medicine, Department of Surgery and Cancer, Faculty of  
Medicine, Imperial College London, SW7 2AZ, London, UK.



## Bovine Muscle Tissue

Red Solid (30  $\mu$ l HRMAS); black Dashed (692 nl MACS)

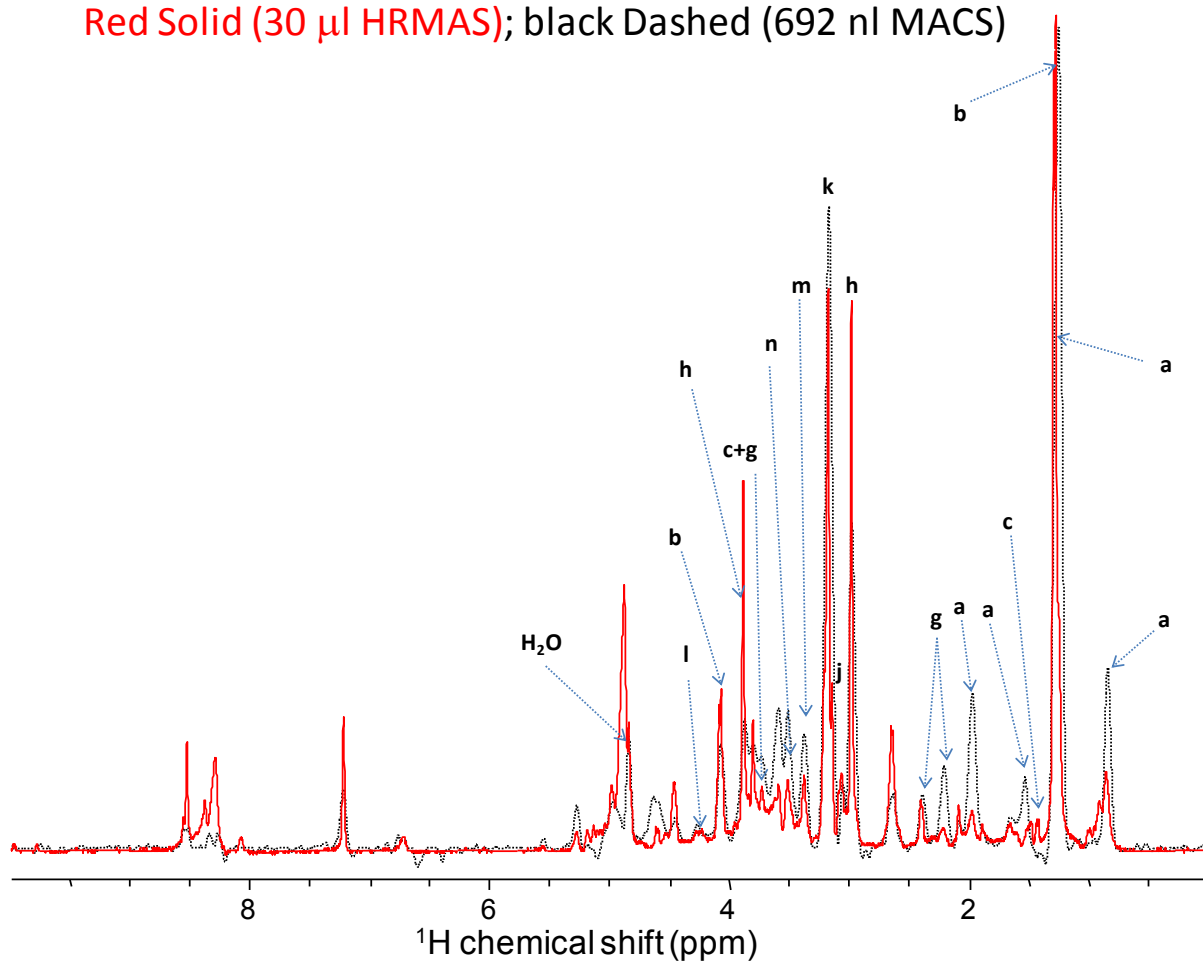


**Figure S1.**  $^1\text{H}$  water-suppressed CPMG NMR spectra of bovine muscle tissue. The red solid spectrum represents the 30  $\mu$ l bulk sample measured with HR-MAS and the black dashed spectrum represents the 692 nl sample measured with MACS. The peak assignments are indicated by the labels a-p (the key is given in Table S1).

## Human Gastric Tumour Tissue

Red Solid (30  $\mu$ l HRMAS); black Dashed (692 nl MACS)

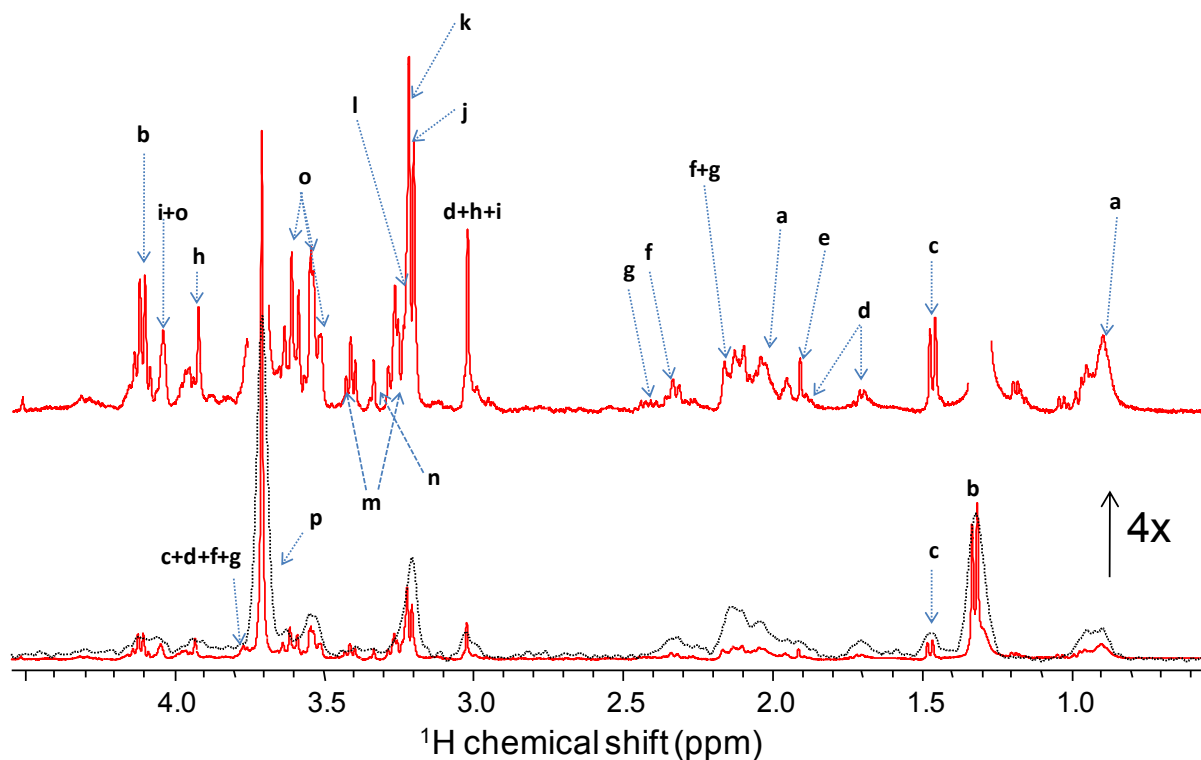


**Figure S2.**  $^1\text{H}$  water-suppressed CPMG NMR spectra of human gastric tumor tissue. The red solid spectrum represents the 30  $\mu$ l bulk sample with HR-MAS and the black dashed spectrum represents the 692 nl sample with MACS. The peak assignments are indicated by the labels a-p (the key is given in Table S1).

**Table S1.** Spectral assignment for the  $^1\text{H}$  NMR spectrum of bovine muscle and human gastric mucosa tissue (Figures S1 & S2)

Label	Metabolite	Chemical Shift [ppm] (Multiplicity) <sup>1</sup>
<b>a</b>	Lipids <sup>2</sup>	0.9 (m), 2.00 (m), 5.28 (m), 5.44 (m)
<b>b</b>	Lactate	1.32 (d), 4.11 (q)
<b>c</b>	Alanine	1.47 (d), 3.76 (q)
<b>d</b>	Lysine	1.47 (m), 1.71 (m), 1.89 (m), 3.02 (t), 3.74 (t)
<b>e</b>	Acetate	1.91 (s)
<b>f</b>	Glutamate	2.04 (m), 2.12 (m), 2.35 (m), 3.75 (dd)
<b>g</b>	Glutamine	2.13 (m), 2.44 (m), 3.77 (t)
<b>h</b>	Creatine	3.04 (s), 3.93 (s)
<b>i</b>	Creatinine	3.03 (s), 4.05(s)
<b>j</b>	Choline	3.21 (s), 3.51 (m), 4.06 (m)
<b>k</b>	Phosphorylcholine	3.22 (s), 3.59 (t), 4.16 (m)
<b>l</b>	Glycerophosphocholine	3.23 (s), 3.63 (m), 3.90 (m), 4.3 (m)
<b>m</b>	Taurine	3.25 (t), 3.42 (t)
<b>n</b>	Scyllo-inositol	3.34 (s)
<b>o</b>	Myo-inositol	3.27 (t), 3.53 (dd), 3.62 (t), 4.05 (t)
<b>p</b>	PEG	3.70 (s)

<sup>1</sup> Abbreviations and Key: d, doublet; dd, doublet of doublets; t, triplet; q, quartet; m, multiplet.

<sup>2</sup> In the gastric mucosa tumor tissue, triglycerides are the main molecules observed in the lipid signal (Wang, Y.; Holmes, E.; Comelli, EM.; Fotopoulos, G.; Dorta, G.; Tang, H.; Rantalainen, MJ.; Lindon, J.C.; Corthésy-Theulaz, I.E.; Fay, L.B.; Kochhar, S.; Nicholson, J.K. *J Proteome Res* **2007**, *6*, 3944-3951.).

**Human Gastric Tumour Tissue (692 nl MACS)**  
Red Solid NOESY pre-sat; Black Solid CPMG pre-sat

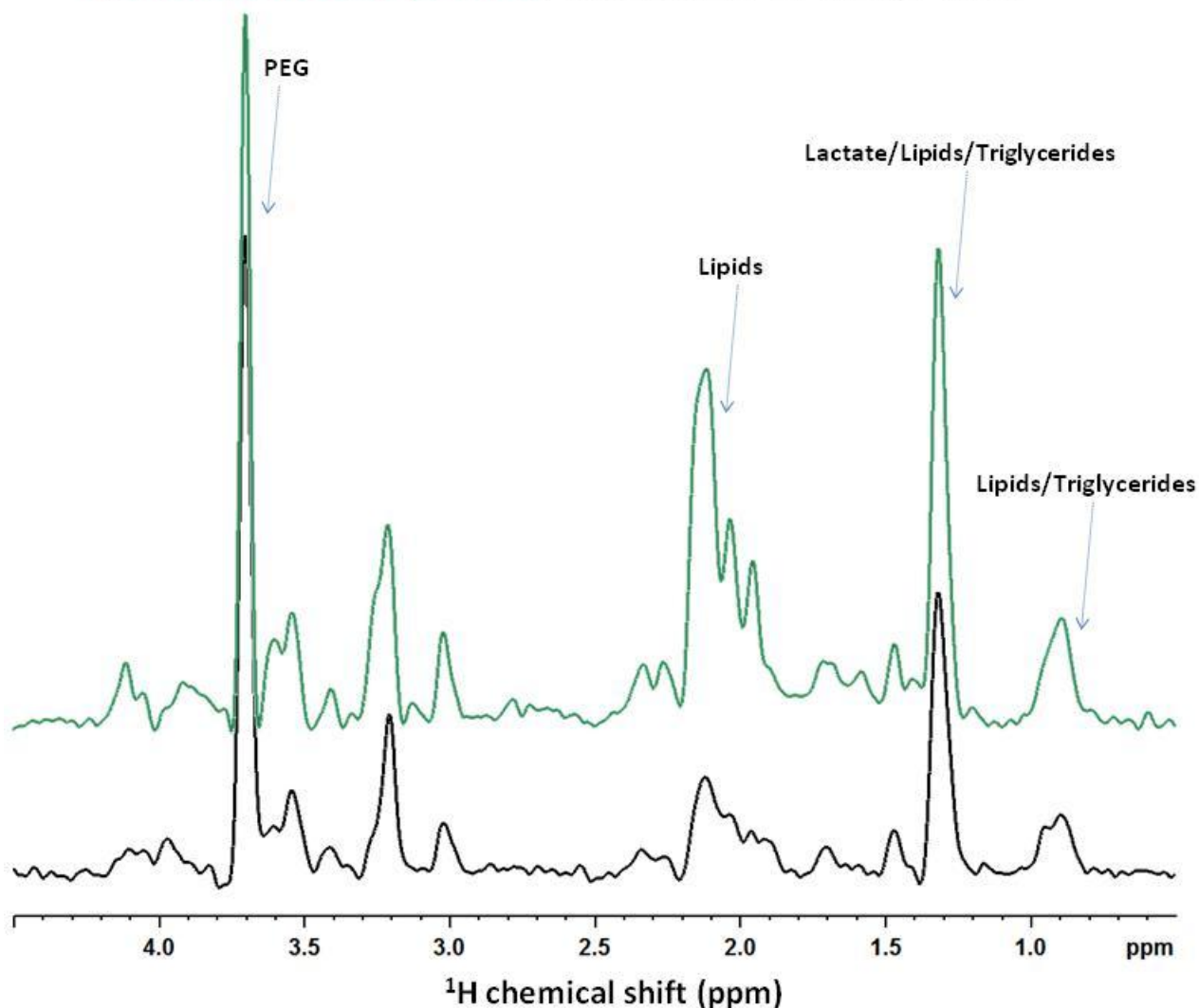


**Figure S3.**  $^1\text{H}$  water-suppressed NOESY (green) and CPMG (black) NMR spectra of human gastric tumor tissue. The two spectra have been recorded with using recycling delays of 2 s and acquisition times of 2.7 s. 1k scans were accumulated and the spectral width was set at 30 ppm with the center in the water signal.

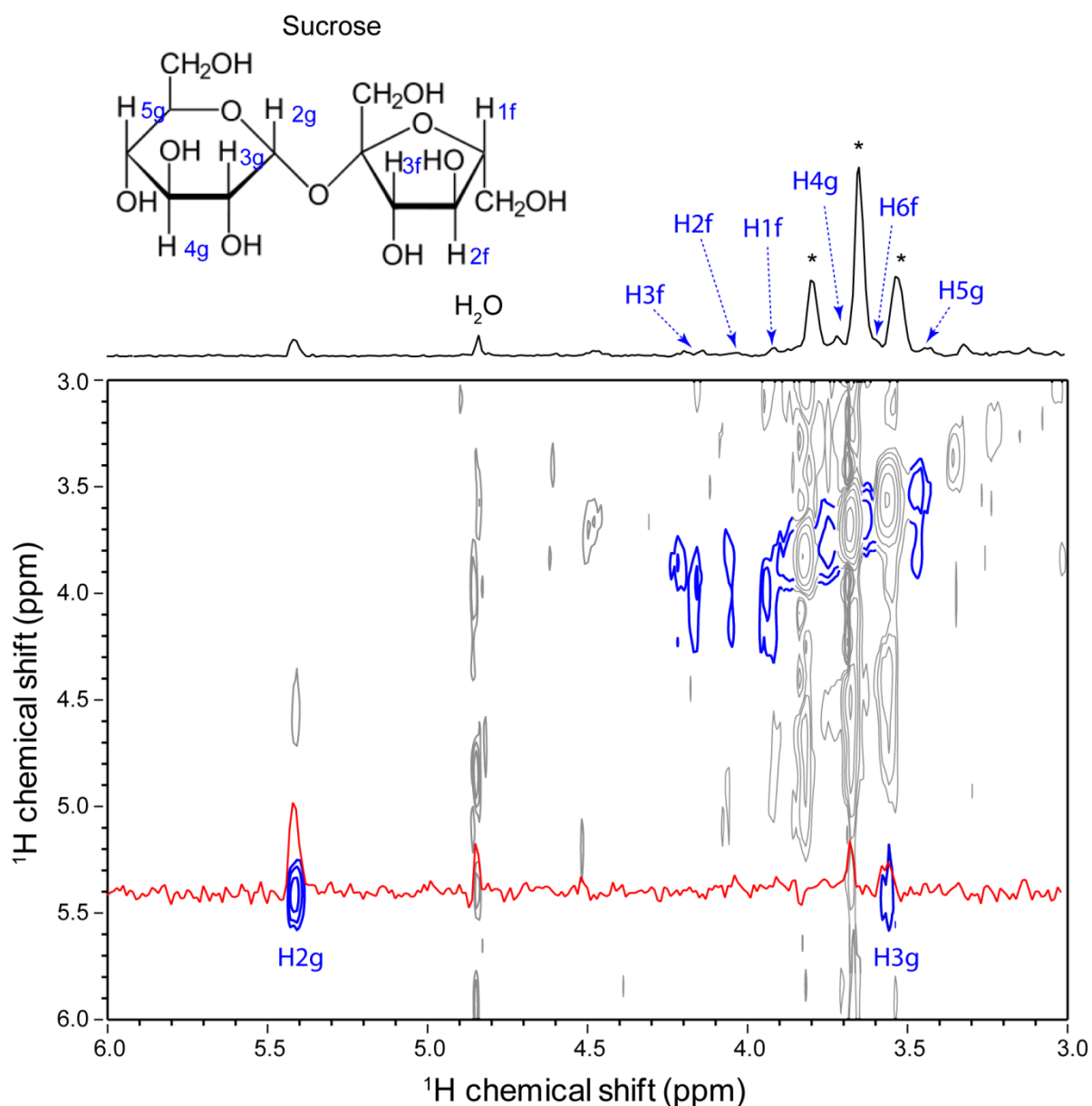


**Figure S4.**  $^1\text{H}$  2D TOCSY spectrum of a 692 nl 2 mM sucrose solution. Peaks from a wax impurity, probably from the paraffin wax used for sealing the capillary, are marked with asterisks in the top projection. These intense signals are overlapped with some of the sucrose signals, revealing only part of the sucrose TOCSY spectrum (high-lighted in blue). As shown clearly in the red insert projection spectrum, the sucrose  $\text{H}_{2g}$  (at 5.47 ppm) is coupled to  $\text{H}_{3g}$  (at 3.58 ppm) [please refer to the H-labels to the top insert sucrose molecule]. The cross peaks of some fructose signals ( $\text{H}_{1f}$ ,  $\text{H}_{2f}$ ,  $\text{H}_{3f}$ ) are also observed in the spectrum. The TOCSY mixing time for the homonuclear Hartman-Hahn transfer was 50 ms. The spin-lock was



achieved by a DIPSI2 pulse sequence train. A spectral width of 4100 Hz was used and the total acquisition time was about 16 h.